Ecological Indicators 114 (2020) 106308

Contents lists available at ScienceDirect

Ecological Indicators

journal homepage: www.elsevier.com/locate/ecolind

Optimal configuration of stand structures in a low-efficiency *Robinia pseudoacacia* forest based on a comprehensive index of soil and water conservation ecological benefits

Guirong Hou[a,d], Huaxing Bi[a,b,c,d,e,f,*], Xi Wei[g], Ning Wang[a], Yanhong Cui[a], Danyang Zhao[a], Xiaozhi Ma[a], Shanshan Wang[a]

[a] College of Soil and Water Conservation, Beijing Forestry University, Beijing 100083, China
[b] Forest Ecosystem Studies, National Observation and Research Station, Jixian, Shanxi 042200, China
[c] Beijing Collaborative Innovation Centre for Eco-environmental Improvement with Forestry and Fruit Trees, China
[d] Key Laboratory of State Forestry Administration on Soil and Water Conservation (Beijing Forestry University), 100083 Beijing, China
[e] Beijing Engineering Research Centre of Soil and Water Conservation (Beijing Forestry University), 100083 Beijing, China
[f] Engineering Research Centre of Forestry Ecological Engineering, Ministry of Education (Beijing Forestry University), 100083 Beijing, China
[g] College of Forestry, Shanxi Agricultural University, 030800 Taigu, China

ARTICLE INFO

Keywords:
Stand structures
Soil and water conservation
Stand density
Optimization
Robinia pseudoacacia

ABSTRACT

The optimization of the stand structures of low-efficiency forests is often required to sustainably achieve the full range of ecological benefits from soil and water conservation in forests. This study was conducted in the Caijiachuan watershed of the Loess Plateau in western Shanxi, China, and explored the practical, and optimal configuration of stand structures in a *Robinia pseudoacacia* forest. Accordingly, one hundred and ninety-five standard plots (20 × 20 m^2), including six stand densities (~500, ~1000, ~1500, ~2000, ~2500 and ~3000 plants·hm^{-2}), were established. Twenty functional indicators and ten structural indicators were monitored and investigated from June to September each year from 2017 to 2018. The results suggested that the forest was divided into three levels of low efficiency, which were mild (II), moderate (III), and severe (IV), based on the soil and water conservation ecological benefits index (SWBI). The trends of the polarization of the values of the stand structure indicators appeared in forests II, III and IV, and this phenomenon became increasingly obvious with increasing levels of low efficiency. Analysis of the influence factors indicated that the climate of this region exhibited a warming and drying trend, the soil moisture content presented a decreasing trend, and the vegetation growth rate slowed. The stand density (SD), tree height (TH), canopy density (CD) and the leaf area index (LAI) were the main controllable factors that influenced the low SWBI of the *R. pseudoacacia* forest. The results of the optimal configuration of the stand structure suggested that the SD should be controlled between 1000 and 1600 plants·hm^{-2}, the TH should be controlled between 7 and 9 m, the CD should be controlled between 0.6 and 0.8, and the LAI should be controlled between 2.5 and 5. In comparison to the SWBI of the existing stand structure configuration, the optimal configuration is expected to improve the SWBI by approximately 86%, 200% and 600% in *R. pseudoacacia* forests I, II and III, respectively. These results will provide a more scientific and complete reference for the optimization of the stand structures of low-efficiency *R. pseudoacacia* forests.

1. Introduction

Afforestation, which has gained significant attention, is an effective measure to stop, reverse and improve damaged and fragile ecological environments (García-Ruiz, 2010). Forests for soil and water conservation are widely used to improve the ecological conditions in arid and semiarid regions and are the main components of the Three-North Shelterbelt Project, known as the "Green Great Wall" of China (Cheng et al., 2014; Wang and Zhou, 2003). *Robinia pseudoacacia* is a pioneer tree species that is used to control soil and water loss on the Loess Plateau and in other arid and semiarid regions, as these trees have high survival rates, can withstand drought, grow rapidly, and have been widely planted (Meng, et al., 2016; Vítková, et al., 2017). However, the soil and water conservation functions of *R. pseudoacacia* forests on the

* Corresponding author at: College of Soil and Water Conservation, Beijing Forestry University, Beijing 100083, China.
E-mail address: bhx@bjfu.edu.cn (H. Bi).

https://doi.org/10.1016/j.ecolind.2020.106308
Received 24 July 2019; Received in revised form 4 March 2020; Accepted 9 March 2020
Available online 18 March 2020
1470-160X/

Loess Plateau and in arid and semiarid regions in China have gradually weakened (Singh et al., 2001). If this low-efficiency phenomenon continues to occur, then a series of serious ecological environmental issues will occur. Therefore, low-efficiency *R. pseudoacacia* forests should have reasonable stand structure adjustments implemented as soon as possible to maintain their main ecological function, i.e., soil and water conservation.

Decreased vegetation coverage results in bare soil surface, which can cause wind erosion (Zhang et al., 2017), serious soil and water loss after rainfall, and some other geological hazards such as debris flow disasters, landslide hazards, and collapse, which increases the risks to humans, accelerating the loss of valuable animals and vegetation (Ma et al., 2016; Ma et al., 2017). To mitigate this problem, the Chinese government implemented a variety of measures. In particular, vegetation coverage improved after the Grain for Green Project was implemented, and the frequencies of geological hazards have greatly decreased, as economic development in China has rapidly increased (Li et al., 2002; Meng, et al., 2016; Ouyang et al., 2016). However, traditional forest management, with the aim of maximizing timber production or maximizing vegetation coverage rates, does not consider a balanced supply of forest ecosystem services (FESs) (Ahmad et al., 2018), such as the balance of water resource inputs and outputs and the balance of nutrients absorbed and consumed, to meet the increasing and diverse service demands of society (Wang et al., 2015; Wang et al., 2017). Therefore, these afforestation projects easily resulted in relatively high planting densities, and previous studies have indicated that some ecological environmental issues have gradually appeared after many years of vegetation restoration.

Wang et al. (2016) and Wei et al. (2018) suggested that the available soil moisture content often shows a decreasing trend because the shallow soil moisture is insufficient for vegetation growth, while deeper soil moisture is progressively decreasing in *R. pseudoacacia* forest. These changes have resulted in soil drying and increases in soil evaporation and vegetation transpiration. Soil moisture is the foundation of ecosystem sustainability in arid and semiarid regions (Liu et al., 2020), and it can benefit land use management in water-shortage regions such as the Loess Plateau of China (Gao et al., 2013). Liang et al. (2018) suggested that the depth-averaged soil moisture content (SMC) was generally lower in forest sites than in cropland sites, both in the shallow layers and in the deep profiles. These authors believe that compared with the native vegetation, the introduced *R. pseudoacacia* plantations caused intense reductions in soil moisture. The implementation of a vegetation restoration project has a significant role in promoting the control of soil and water loss (Ludwig et al., 2005; Xin et al., 2015; Duan et al., 2017). Any vegetation, if overplanted, will disrupt the balance of water resources, especially in areas below the 500–550 mm precipitation threshold (Liang et al., 2018). One possible reason why soil moisture declined following the planting of *R. pseudoacacia* is that planation density is greater than the soil water and vegetation carrying capacity (Deng et al., 2012; Wang et al., 2016; Liang et al., 2018). Therefore, an optimal configuration of vegetation is an effective measure to reverse and improve ecological environmental issues.

Planted *R. pseudoacacia* was not an incorrect choice in arid and semiarid regions; however, the improper stand structure used has resulted in the degradation of the main ecological function of the forest. Thus, some of the healthy forests changed to low-efficiency forests. It is necessary to address improper existing stand structures to maintain the important role of soil and water conservation functions in these areas, as structure determines function (Pukkala et al., 2010; Jiang et al., 2017). The indexes of horizontal forest structure include diameter at breast height (DBH), the crown index, stand density (SD), canopy density (CD), the uniform angle index, the scale size ratio, and the competition index; the indexes pertaining to vertical forest structure include tree height (TH), the leaf area index (LAI), the forest layer index (FLI), and stand porosity (Hui et al., 2007). Among these stand structure indexes, SD affects all the other stand structure indexes. When the SD is optimized, it will affect the other stand structure indexes, and optimizing SD has strong maneuverability (Li et al., 2012). Therefore, optimizing stand structure is approximately equal to optimizing SD.

Therefore, three hypotheses are identified in this study. The first hypothesis is that some low-efficiency *R. pseudoacacia* forests exist among the existing *R. pseudoacacia* forests, but not all of them exhibit low efficiency. Second, the decrease in precipitation, the increase in temperature and unreasonable stand structures promote the formation of low-efficiency *R. pseudoacacia* forests. Third, a proper optimal vegetation configuration exists that can improve the stand structures of existing low-efficiency *R. pseudoacacia* forests as well as the soil and water conservation ecological benefits. Accordingly, in this study, we first attempt to propose a set of appropriate optimal configurations for different *R. pseudoacacia* forests with different levels of low efficiency to address the gap in low-efficiency improvements. The Caijiachuan watershed on the Loess Plateau in western Shanxi was selected as the study site, and *R. pseudoacacia* was selected as the study species (planted from 1990 to 1995).

Therefore, the main objectives of this study were to (1) propose a method for determining the levels of low efficiency in the R. pseudoacacia forest by constructing a soil and water conservation ecological benefits index (SWBI), (2) apply a trend analysis and structural equation model (SEM) to analyze the factors influencing each level of low efficiency in R. pseudoacacia forests according to climate and stand structures and (3) determine the optimal configuration of the stand structure in *R. pseudoacacia* forests according to the results of the response surface method (RSM).

2. Materials and methods

2.1. Site description

The Caijiachuan watershed served as the study site; this watershed is located on the Loess Plateau in Ji County, Shanxi Province, China (Fig. 1), and is a typical gully area. Meteorological records indicate that the long-term mean annual air temperature is 10.2 °C and the frost-free period is 172 days. The average annual precipitation is 571 mm, with an uneven distribution. The average annual potential evapotranspiration (PET) is 1724 mm, which far exceeds the rainfall. Inside this area, the type of soil is mainly Haplic Luvisols (soil classification of the Food and Agriculture Organization of the United Nations) and is mostly alkaline. There are mainly artificial shelterbelts of black locust (*Robinia pseudoacacia* L.) and Chinese pine (*Pinus tabulaeformis* Carr.) in the nested watershed, with an area of 38 km^2 and a forest cover rate of 72%. Any deforestation must be approved by the forestry bureau, and no land reclamation is allowed. This study established one hundred and ninety-five standard plots (20 × 20 m^2) that included six stand densities (~500, ~1000, ~1500, ~2000, ~2500 and ~3000 plants·hm^{-2}) from June to September of each year from 2017 to 2018 according to the statistical information regarding *R. pseudoacacia* forestland provided by the Ji County, Forestry Bureau of Linfen City, Shanxi Province, which covered almost all *R. pseudoacacia* forestland in this watershed (Fig. 1). Basic information on a standard *R. pseudoacacia* forestland is shown in Table 1.

2.2. Climate data

The climate (precipitation and air temperature) data (1957–2018 year) used in this study were downloaded from the State Meteorological Administration of China (daily data sets of surface climatological information in China (V3.0)) and applied to analyze the change trends of precipitation and air temperature in this study area through the Mann-Kendall statistical test. The detailed theoretical method refers to Zhao et al. (2017). The precipitation and air temperature data were monitored by a synoptic station in Ji County (station index number: 83859, E: 110°01′50″, N: 36°05′). The Mann-Kendall

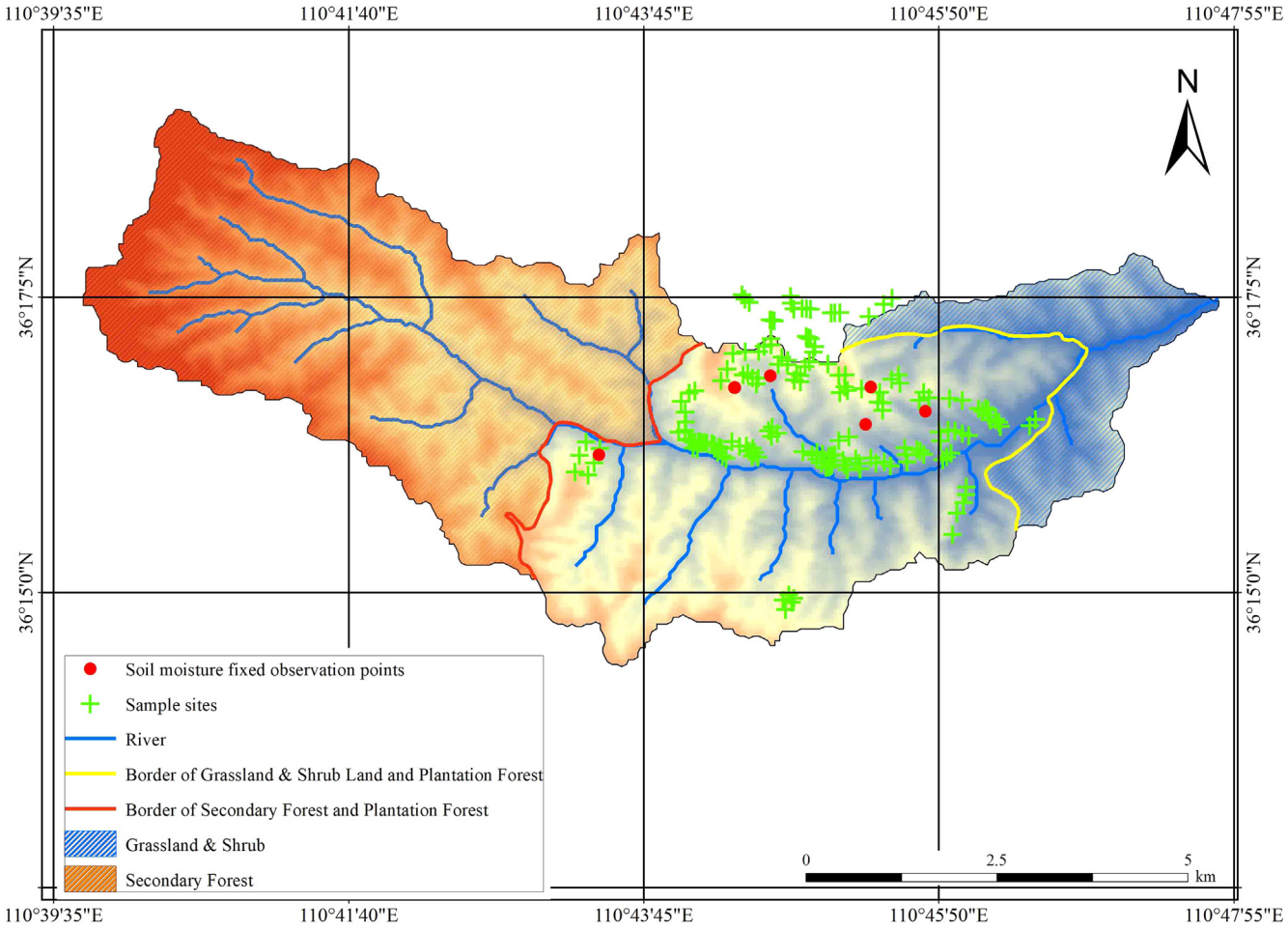

Fig. 1. Distribution of the sample plots in the Caijiachuan watershed on the Loess Plateau.

statistical test was conducted using MATLAB R2014a (The Math Works, Natick, MA, USA) in this study.

2.3. Investigation of stand structure and soil and water conservation indicators

In this paper, stand structure indicators include diameter at breast height (DBH), tree height (TH), tree crown area (CA), stand density (SD), canopy density (CD), the leaf area index (LAI), the forest layer index (FLI), angle scale (AS), tree competition index (TCI), and tree size ratio (SR). Using individual field measurements in these plots, DBH, TH, and CA were measured; then, the SD, CD, FLI, AS, TCI, and SR were calculated. Refer to Hui et al. (2007) for the detailed theoretical methods. The LAIs of the standard plots were determined using a LAI-2000 (LI-COR Company, Lincoln, NE, USA) vegetation canopy analyzer. The stand structure indicators that have main effects on the SWBI were used to analyze the characteristics of distribution with the following four density functions, exponential, Weibull, lognormal and gamma (Table 2).

Table 2
Four density functions of probability distribution.

Distribution	Density function	Parameter
Exponential	$f(x) = \lambda \exp(-\lambda x)$	λ: Scale parameter
Weibull	$f(x) = \frac{\gamma}{\beta}\left(\frac{x}{\beta}\right)^{\gamma-1} \exp(-\frac{x}{\beta})^{-2}$	γ: Shape parameter β: Scale parameter
Lognormal	$f(x) = \frac{1}{\sqrt{2\pi}\sigma} exp\left[\frac{-(\log(x)-\mu)}{2\sigma^2}\right]$	μ: The mathematical expectation of the random variable log(x) σ: The standard deviation of the random variable log(x)
Gamma	$f(x) = \frac{x^{\alpha-1}}{\beta^{\alpha}\Gamma(x)} \exp(-\frac{x}{\beta})$	α: Shape parameter β: Scale parameter

In this paper, to explore the practical and optimal configuration of stand structures in a *Robinia pseudoacacia* forest to improve the soil and water conservation ecological benefits of the low-efficiency forest, two

Table 1
Basic information on a standard *R. pseudoacacia* forest.

Stand density (plants·hm^{-2})	Elevation (m)	Slope (°)	Av. tree height (m)	Av. DBH (cm)	Av. tree age (a)	Leaf area index
~500	1170	22	6.8 ± 1.19	7.5 ± 0.09	25	1.61
~1000	1180	39	9.7 ± 1.61	13.9 ± 0.28	26	1.78
~1500	1190	22	8.6 ± 1.06	10.5 ± 0.31	25	1.98
~2000	1180	23	9.5 ± 1.37	9.6 ± 0.55	22	2.74
~2500	1120	15	8.7 ± 1.63	9.6 ± 0.69	23	3.24
~3000	1120	26	7.8 ± 1.96	8.8 ± 0.65	23	3.91

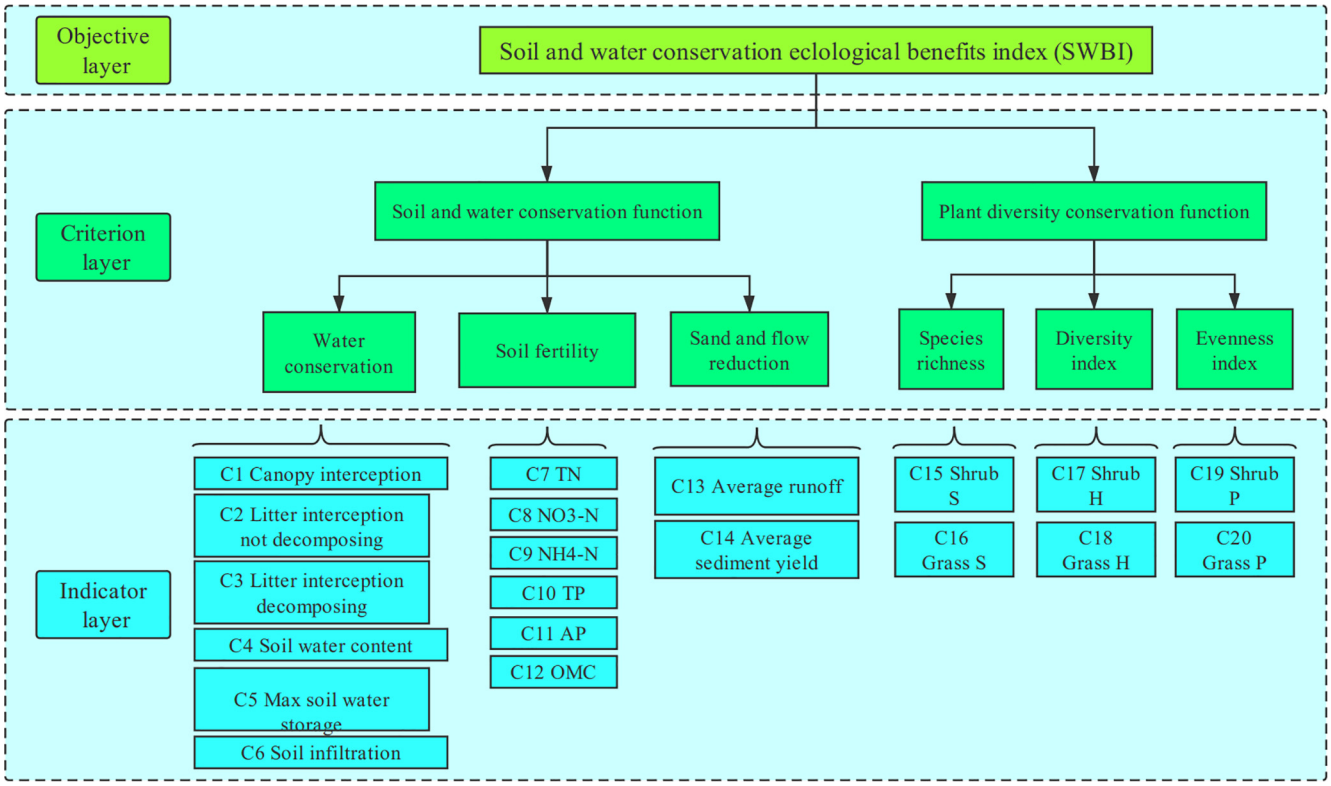

Fig. 2. Index system of the comprehensive evaluation of the soil and water conservation ecological benefits of the *R. pseudoacacia* forest.

main ecological functions were focused on—soil and water conservation and understory plant diversity conservation. Accordingly, twenty indicators that represent the two main ecological functions were selected to construct the soil and water conservation ecological benefits index (Fig. 2). These indicators include canopy interception rate, litter interception rate, SMC, maximum soil water storage content, soil infiltration rate, soil total nitrogen content (TN), soil ammonia-nitrogen (NH_3-N), soil nitrate-nitrogen (NO_3-N), soil total phosphorus (TP), and soil available phosphorus (AP), soil organic matter contents (OMC), average runoff, average sediment yield, species richness, diversity index, and evenness index. Mixed soil samples, 0–400 cm, were collected using a soil auger and were representative of the forest soils in this area; the SMC was determined using the drying method; and soil water infiltration capacity was measured using a soil infiltration method. After air-dried soil was sieved (0.15 mm sieve), indoor experiments were conducted. TN, NH_3-N, NO_3-N, TP, and AP were measured with a SmartChem-200 (AMS/Alliance Instruments, Paris, France) discrete wet chemistry analyzer, and the potassium dichromate dilution heat method was applied to measure the OMC of the soil samples.

2.4. Statistical analysis

2.4.1. Determining the classifications of the low-efficiency R. pseudoacacia forest

The comprehensive coordinate evaluation method was employed to assess the soil and water conservation ecological benefits of the *R. pseudoacacia* forest on soil and water conservation functions and plant diversity protection functions, and the evaluation factor system is shown in Fig. 2.

First, dimensionless processing was carried out for all data, and the original data table was represented as X_{ij}, where i indicated the number of sample plots and j indicated all the evaluation factors. Second, each data point was compared to the maximum value (X_j) for that index to construct the matrix coordinate as represented by d_{ij} using the following Eq. (1):

$$d_{ij} = \frac{X_{ij}}{X_j} \tag{1}$$

The distance of the i index from the standard point was then calculated using Eq. (2), and the next step was to calculate the sum of the distances of each treatment to the standard point using Eq. (3). Finally, the order was ranked according to the M value, and the smallest value among the comprehensive results was considered best.

$$p_i = \sqrt{\sum_i (1\text{-}d_{ij})^2} \tag{2}$$

$$M = \sum_{i=1}^{n} p_i \tag{3}$$

where n is the number of indicators evaluated in this study, $n = 20$.

The soil and water conservation ecological benefits comprehensive index (SWBI) of the *R. pseudoacacia* forests was divided into healthy *R. pseudoacacia* forest and low-efficiency *R. pseudoacacia* forest. Determining the threshold of the low-efficiency *R. pseudoacacia* forest was based on the regression relation of every stand structure with SWBI in same weight in this study. The low-efficiency *R. pseudoacacia* forest was divided into three low-efficiency classes, mild, moderate and severe. Accordingly, the SWBI values were divided into three ranges according to an arithmetic progression (a_1, a_2, a_3, a_4), i.e., $a_1 \sim a_2$, $a_2 \sim a_3$, $a_3 \sim a_4$ represent three health statuses (I, mild level of low efficiency; II, moderate level of low efficiency; and III, severe level of low efficiency) of the *R. pseudoacacia* forest. The minimum and maximum values of M were 0.96 and 9.04, respectively, according to Eq. (3), which can deduced that the range of SWBI was 0–10 in this study. The new matrix of M' changed according to Eq. (4); the order was ranked according to the M' value, and the larger value among the comprehensive results was considered better.

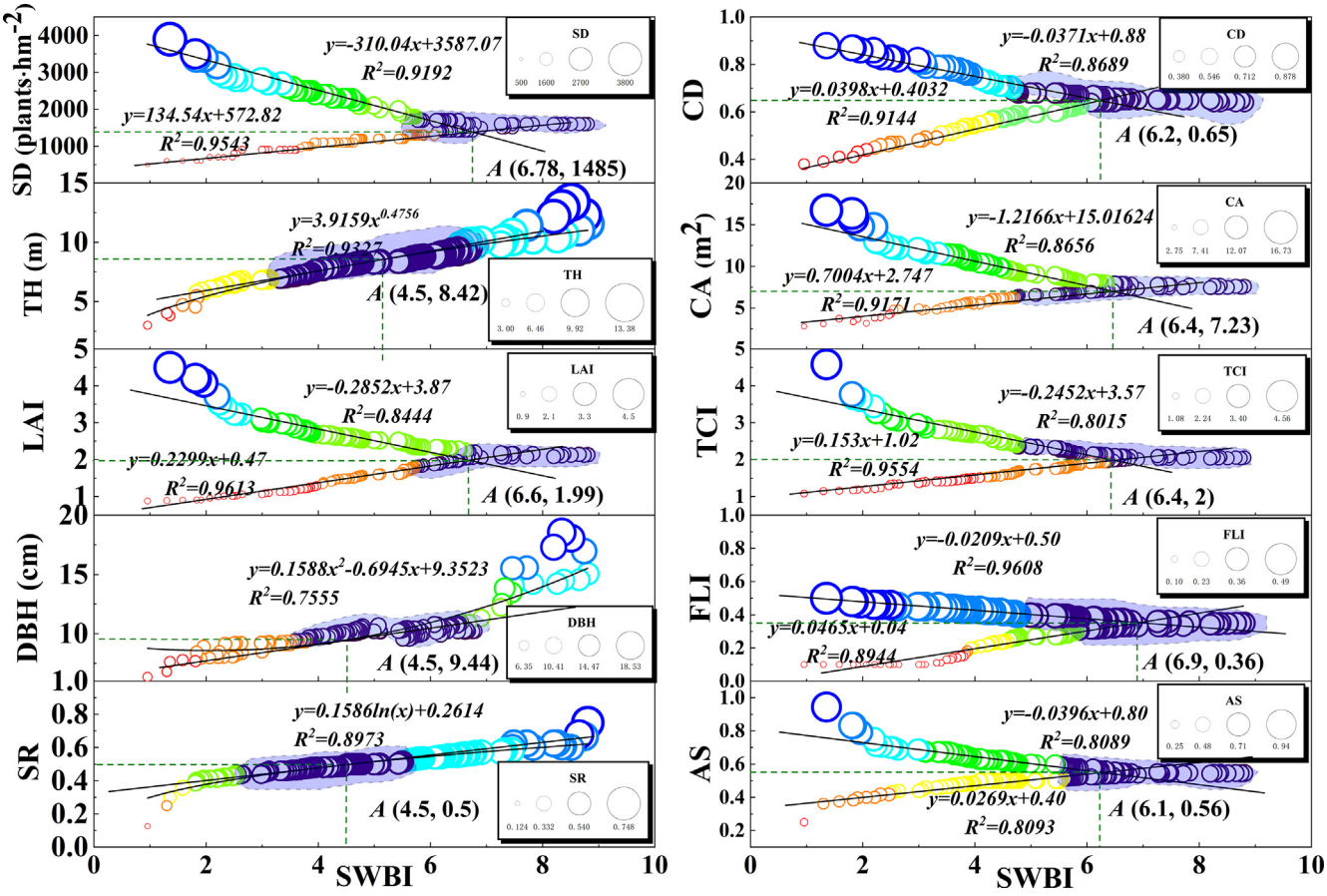

Fig. 3. Determination of the threshold of *R. pseudoacacia* forest based on the SWBI.

$$M' = 10 - \sum_{i=1}^{n} p_i \tag{4}$$

2.4.2. Measurement of the soil moisture content and calculation of the volume growth rate of wood

There are six fixed continuous observation points for the SMC in *R. pseudoacacia* forestland, in which the stand densities are 625, 1125, 1475, 1900, 2675, and 3050 plants·hm^{-2}, respectively (Fig. 1), and the corresponding data were applied to analyze the various trends of the SMC during vegetation restoration in this study. The SMC was measured with a time-domain reflectometer (TDR) soil moisture meter to the soil depth of 200 cm (one layer per 20 cm) on the 10th, 20th and 30th days of each month from 2005 to 2018.

A standard wood sample was selected and cut from each of the six fixed observation points to analyze the volume growth rate of *R. pseudoacacia* forests during vegetation restoration based on the data of the growth rings of the wood, and the rate was calculated using the following Eqs. (5) and (6):

$$V = L \times \sum_{i=1}^{n} g_i + \frac{1}{3} \times g' \times L' \tag{5}$$

$$P_v = \frac{V_a - V_{a-n}}{V_a + V_{a-n}} \times \frac{200}{n} \tag{6}$$

where V is volume of wood in the standard wood samples at different ages (m^3); L is the length of each segment of the standard wood sample (m); g_i is the central sectional area of segment i of the standard wood (m^2); g' is the bottom sectional area of the tree top of the standard wood sample (m^2); L' is the length of the tree top of each standard sample (m); P_v is the volume growth rate (%); and n is the forest age.

2.4.3. Analysis of the relationship between the stand structure and the SWBI of the low-efficiency R. pseudoacacia forest

To identify the factors that have the main effects on SWBI and provide the basis for further optimization of the stand structure of low-efficiency *R. pseudoacacia* forest, a SEM was employed to analyze the relationship of the stand structure and SWBI of the low-efficiency *R. pseudoacacia* forest in this paper. Amos software (ver. 22.0, IBM/International Business Machines Corporation, Armonk, NY, USA) was used to construct the SEM in this study. The SEM includes two parts, the measurement model and the structural model; the formulas are as follows (7)–(9):

$$X = \Lambda_x \xi + \delta \tag{7}$$

$$Y = \Lambda_y \eta + \varepsilon \tag{8}$$

$$\eta = B\eta + \Gamma\xi + \zeta \tag{9}$$

where X is the exogenous observation variable vector, Y is the endogenous observation variable vector, Λ_x and Λ_y are the factor loadings of the indicator variables (X, Y), δ and ε are the measurements of the exogenous observation variables and the endogenous observation variables, ξ is the exogenous latent variable, and η is the endogenous latent variable. B is the structural coefficient matrix of the relationship between endogenous latent variables, Γ is the structural coefficient matrix of the relationships between endogenous latent variables and exogenous latent variables, and ζ is the interference factor or residual value of the structural model.

2.4.4. Optimization of stand structures of low-efficiency R. pseudoacacia forests

The response surface methodology was employed to optimize the stand structure of a *R. pseudoacacia* forest under conditions of mild

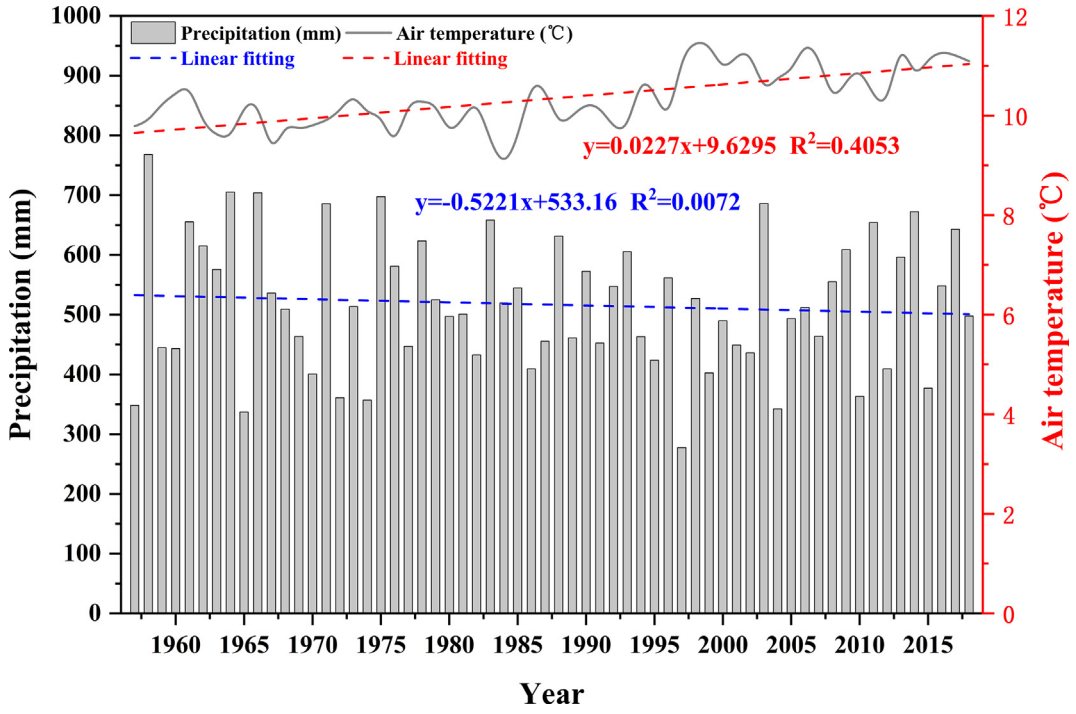

Fig. 4. Annual precipitation and air temperature in Jixian County during 1957–2018.

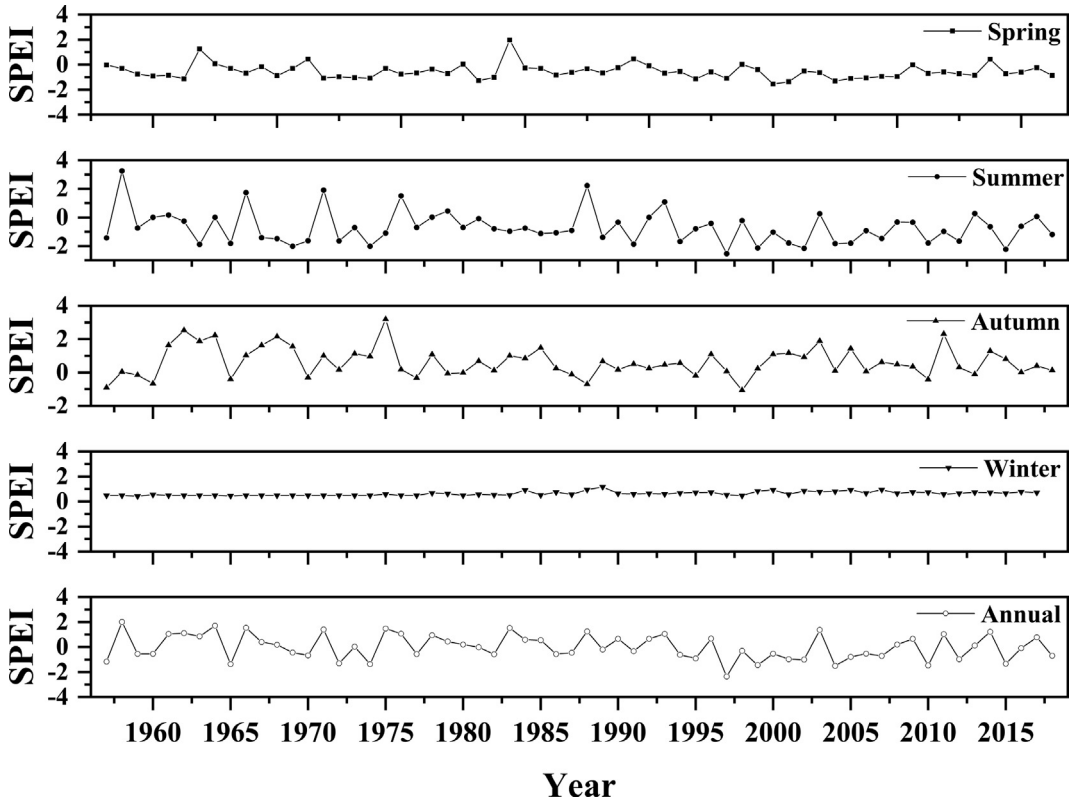

Fig. 5. Corresponding seasonal and annual SPEI of each year from 1957 to 2018 in the study area.

degradation, moderate degradation and severe degradation. The response surface methodology (RSM) was performed with SAS (version 9.1, SAS Institute Inc., Cary, NC). The formula for the response surface methodology is as follows (10):

$$y(x) = \beta_0 + \sum_{i=1}^{p} \beta_i X_i + \sum_{i=1}^{p} \sum_{j=1, i<j}^{p} \beta_{ij} X_{ij} + \sum_{i=1}^{p} \beta_{ij} X_i^2 + \varepsilon \quad (10)$$

where X_i is the independent variable, $y(x)$ is the response value, β_0 is the constant term, β_i is the linear effect, β_{ij} is the interaction effect, ε is the error term.

Fig. 1 was generated with ArcGIS 10.1 (Environmental Systems

Table 3
Evaluation results of the SWBI of the *R. pseudoacacia* forest.

Number	SWBI	Number	SWBI	Number	SWBI	Number	SWBI	Number	SWBI
1	8.26	40	6.77	79	6.79	118	5.12	157	6.62
2	7.82	41	6.5	80	6.75	119	4.09	158	6.43
3	7.71	42	6.48	81	4.97	120	3.05	159	6.3
4	7.48	43	6.45	82	2.55	121	1.11	160	6.09
5	6.59	44	6.44	83	2.53	122	6.72	161	6.1
6	6.58	45	4.12	84	2.5	123	0.96	162	6.88
7	5.53	46	6.65	85	6.38	124	7.27	163	6.55
8	9.04	47	6.63	86	6.36	125	6.69	164	6.46
9	6.11	48	5	87	6.35	126	1.3	165	6.66
10	5.86	49	6.52	88	6.33	127	2.32	166	6.65
11	6.86	50	6.51	89	6.69	128	4.94	167	6.67
12	6.5	51	6.51	90	6.67	129	7.45	168	6.47
13	8.34	52	6.51	91	6.65	130	7.46	169	6.61
14	1.81	53	6.14	92	6.64	131	7.32	170	6.16
15	1.58	54	6.13	93	6.62	132	6.68	171	2.49
16	1.35	55	6.11	94	6.69	133	2.21	172	4.83
17	6.44	56	6.07	95	6.61	134	2.24	173	6.58
18	6.36	57	4.49	96	6.59	135	2.19	174	6.75
19	6.32	58	5.44	97	1.91	136	2.06	175	1.79
20	6.31	59	6.09	98	1.83	137	6.24	176	2.47
21	6.54	60	6.08	99	8.37	138	5	177	5.58
22	6.5	61	6.22	100	8.2	139	6.24	178	3.53
23	6.49	62	6.2	101	6.99	140	6.68	179	4.86
24	6.49	63	6.18	102	6.79	141	3.83	180	5.39
25	4.39	64	6.16	103	6.78	142	6.74	181	3.34
26	4.34	68	6.6	104	6.77	143	6.65	182	4.82
27	2.98	66	6.56	105	6.71	144	6.76	183	3.8
28	6.72	67	6.52	106	5.82	145	6.73	184	4.77
29	8.74	68	6.51	107	5.8	146	6.45	185	1.32
30	8.65	69	6.74	108	4.77	147	5.93	186	3.12
31	8.51	70	5.75	109	6.31	148	6.49	187	5.59
32	1.95	71	2.64	110	6.3	149	2.34	188	3.12
33	6.22	72	2.63	111	6.26	150	6.52	189	5.49
34	6.18	73	3.71	112	6.24	151	3.88	190	5.44
35	6.09	74	5.68	113	6.69	152	6.62	191	4.75
36	6.09	75	5.63	114	6.67	153	6.07	192	3.68
37	6.85	76	4.6	115	6.67	154	1.85	193	5.63
38	6.82	77	7.25	116	7.3	155	6.5	194	1.6
39	6.79	78	6.91	117	3.32	156	6.52	195	1.97

Research Institute, Inc., Redlands, California, USA). Figs. 3 to 5 were generated with Origin 9.0 software (Origin Lab, Northampton, MA, USA). SPSS software (ver. 25.0, SPSS Inc. Chicago, IL, USA) was used for all statistical analyses in this study.

3. Results

3.1. Determination of the low-efficiency R. pseudoacacia forest

3.1.1. Evaluation of SWBI of the R. pseudoacacia forest

According to Eq. (4), the larger the results of the coordinated comprehensive evaluation are, the better the evaluation result is. Therefore, the comprehensive evaluation result of this study shows that the larger the SWBI is, the better the soil and water conservation ecological benefit of the corresponding *R. pseudoacacia* forest. The evaluation results showed that the maximum and minimum SWBI values of the *R. pseudoacacia* forest were 9.04 and 0.96, respectively (Table 3). Determining the low-efficiency line and levels were important for evaluating the health status of the *R. pseudoacacia* forest based on the SWBI.

3.1.2. Determining the low-efficiency line for the R. pseudoacacia forest

Determining the low-efficiency line for evaluating the *R. pseudoacacia* forest should consider the distribution relationship between each stand structure indicator and the SWBI. Theoretically, in terms of single stand structure, the appropriate SWBIs were different, and Fig. 3 suggested this hypothesis. The corresponding appropriate SWBI value of the stand structures TH, DBH and SR was 4.5. The corresponding appropriate SWBI values of the other stand structures SD, CD, CA, LAI, TCI, FLI and AS were 6.78, 6.2, 6.4, 6.6, 6.4, 6.9 and 6.1, respectively. The weight coefficient was the same in the evaluation process; therefore, all appropriate SWBI values of these ten stand structure indicators were averaged. When the SWBI value was equal to 6, the low-efficiency line was used for the evaluation of the *R. pseudoacacia* forest. *R. pseudoacacia* forests with SWBI values larger than 6 were healthy forests; inversely, *R. pseudoacacia* forests had low-efficiency levels when the SWBI value was less than this score.

Accordingly, the SWBI values were divided into three ranges according to an arithmetic progression (0, 2, 4, 6, d = 2), i.e., 0–2, 2–4, 4–6 represent three health statuses (I, mild level of low efficiency; II, moderate level of low efficiency; and III, severe level of low efficiency) of the *R. pseudoacacia* forest. The low efficiency levels of the *R. pseudoacacia* forest (Table 4) were divided based on the evaluation results of the SWBI of the *R. pseudoacacia* forest (Table 3) and according to the levels of low efficiency. The evaluation results showed that 63.59% of the *R. pseudoacacia* forest was healthy, and the main ecological functions of soil and water conservation and plant diversity protection occurred continuously and steadily. Approximately 16.41% of the *R. pseudoacacia* forest had mild low-efficiency levels in carrying out water and soil conservation functions and plant diversity protection. Although this level of efficiency did not affect coordination between the main ecological functions and stand structure, this kind of forest has a possible trend of degradation, necessitating further stand structure optimization. A moderate level of low efficiency and a severe level of low efficiency accounted for 13.33% and 6.67%, respectively, of the *R. pseudoacacia* forest, indicating that coordination between the soil and

Table 4
Low efficiency levels of the *R. pseudoacacia* forest.

Number	Types	Number	Types	Number	Types	Number	Types	Number	Types
1	Norm.	40	Norm.	79	Norm.	118	L_1	157	Norm.
2	Norm.	41	Norm.	80	Norm.	119	L_1	158	Norm.
3	Norm.	42	Norm.	81	L_1	120	L_2	159	Norm.
4	Norm.	43	Norm.	82	L_2	121	L_3	160	Norm.
5	Norm.	44	Norm.	83	L_2	122	Norm.	161	Norm.
6	Norm.	45	L_1	84	L_2	123	L_3	162	Norm.
7	L_1	46	Norm.	85	Norm.	124	Norm.	163	Norm.
8	Norm.	47	Norm.	86	Norm.	125	Norm.	164	Norm.
9	Norm.	48	L_1	87	Norm.	126	L_3	165	Norm.
10	L_1	49	Norm.	88	Norm.	127	L_2	166	Norm.
11	Norm.	50	Norm.	89	Norm.	128	L_1	167	Norm.
12	Norm.	51	Norm.	90	Norm.	129	Norm.	168	Norm.
13	Norm.	52	Norm.	91	Norm.	130	Norm.	169	Norm.
14	L_3	53	Norm.	92	Norm.	131	Norm.	170	Norm.
15	L_3	54	Norm.	93	Norm.	132	Norm.	171	L_2
16	L_3	55	Norm.	94	Norm.	133	L_2	172	L_1
17	Norm.	56	Norm.	95	Norm.	134	L_2	173	Norm.
18	Norm.	57	L_1	96	Norm.	135	L_2	174	Norm.
19	Norm.	58	L_1	97	L_3	136	L_2	175	L_3
20	Norm.	59	Norm.	98	L_3	137	Norm.	176	L_2
21	Norm.	60	Norm.	99	Norm.	138	L_1	177	L_1
22	Norm.	61	Norm.	100	Norm.	139	Norm.	178	L_2
23	Norm.	62	Norm.	101	Norm.	140	Norm.	179	L_1
24	Norm.	63	Norm.	102	Norm.	141	L_2	180	L_1
25	L_1	64	Norm.	103	Norm.	142	Norm.	181	L_2
26	L_1	68	Norm.	104	Norm.	143	Norm.	182	L_1
27	L_2	66	Norm.	105	Norm.	144	Norm.	183	L_2
28	Norm.	67	Norm.	106	L_1	145	Norm.	184	L_1
29	Norm.	68	Norm.	107	L_1	146	Norm.	185	L_3
30	Norm.	69	Norm.	108	L_1	147	L_1	186	L_2
31	Norm.	70	L_1	109	Norm.	148	Norm.	187	L_1
32	L_3	71	L_2	110	Norm.	149	L_2	188	L_2
33	Norm.	72	L_2	111	Norm.	150	Norm.	189	L_1
34	Norm.	73	L_2	112	Norm.	151	L_2	190	L_1
35	Norm.	74	L_1	113	Norm.	152	Norm.	191	L_1
36	Norm.	75	L_1	114	Norm.	153	Norm.	192	L_2
37	Norm.	76	L_1	115	Norm.	154	L_3	193	L_1
38	Norm.	77	Norm.	116	Norm.	155	Norm.	194	L_2
39	Norm.	78	Norm.	117	L_2	156	Norm.	195	L_3

Table 5
M-K trend test on the precipitation, air temperature and SPEI.

Indicators	Test	Spring	Summer	Autumn	Winter	Annual
Precipitation	Z	−0.85	−0.815	−0.057	5.192**	0.459
Air temperature	Z	4.606**	2.837**	3.354**	3.17**	4.859**
SPEI	Z	−0.976	−1.206	−0.678	5.306**	−0.976

Notes: Z: M-K trend test; ** represents significant test at the 95% level.

water conservation function and plant diversity protection function as well as the stand structure of these two kinds of forest was not high and may even be over lower. It is essential to implement some human intervention measures for stand structure to improve the main ecological function of this forest.

Norm. is the normal forest, L_1 is the *R. pseudoacacia* forest with a mild level of low efficiency, L_2 is the *R. pseudoacacia* forest with a moderate level of low efficiency, and L_3 is the *R. pseudoacacia* forest with a severe level of low efficiency.

3.2. Analysis of the factors influencing the low efficiency of the R. pseudoacacia forest

3.2.1. Changes in rainfall and atmospheric temperature during vegetation restoration

The variation characteristics and statistical test (Mann-Kendall and Spearman) results of the precipitation and annual average temperature in the study area from 1957 to 2018 are shown in Fig. 4. The annual precipitation was 516.71 ± 110.95 mm, the maximum annual precipitation was 768.2 mm, the annual minimum precipitation was 277.6 mm, and the variable coefficient was 0.21. The annual average temperature was 10.34 ± 0.64 ˚C, the annual average temperature varied between 8.95 and 11.59 ˚C, and the variable coefficient was 0.06. Fig. 4 also shows that precipitation and the average temperature presented different degrees of decreases from 1957 to 2018, and Fig. 5 indicates that the standardized precipitation evapotranspiration index (SPEI) also presented decreasing trend from 1957 to 2018.

The results of the M-K trend test on the precipitation, air temperature and SPEI are shown in Table 5. Precipitation presented a significant increasing trend in the winter season (passing the significance test at 95%), while a nonsignificant decreasing trend was displayed in spring, summer, autumn as well as annually. Table 5 also shows that air temperature presented a significant increasing trend during all four seasons and annually (passing the significance test at 95%). The results of the M-K trend test on the SPEI were the same as those for precipitation, as the SPEI presented a significant increasing trend in winter season (passing the significance test at 95%), while it presented a nonsignificant decreasing trend in spring, summer, autumn as well as annually. According to the results of the M-K trend test on the precipitation, air temperature and SPEI, there is a phenomenon of continuous warming and drying in the study area, and this phenomenon is likely to continue for some time.

3.2.2. The change trend of soil moisture content and volume growth rate of wood during the vegetation restoration

The change trends of the SMC and volume growth rate during the

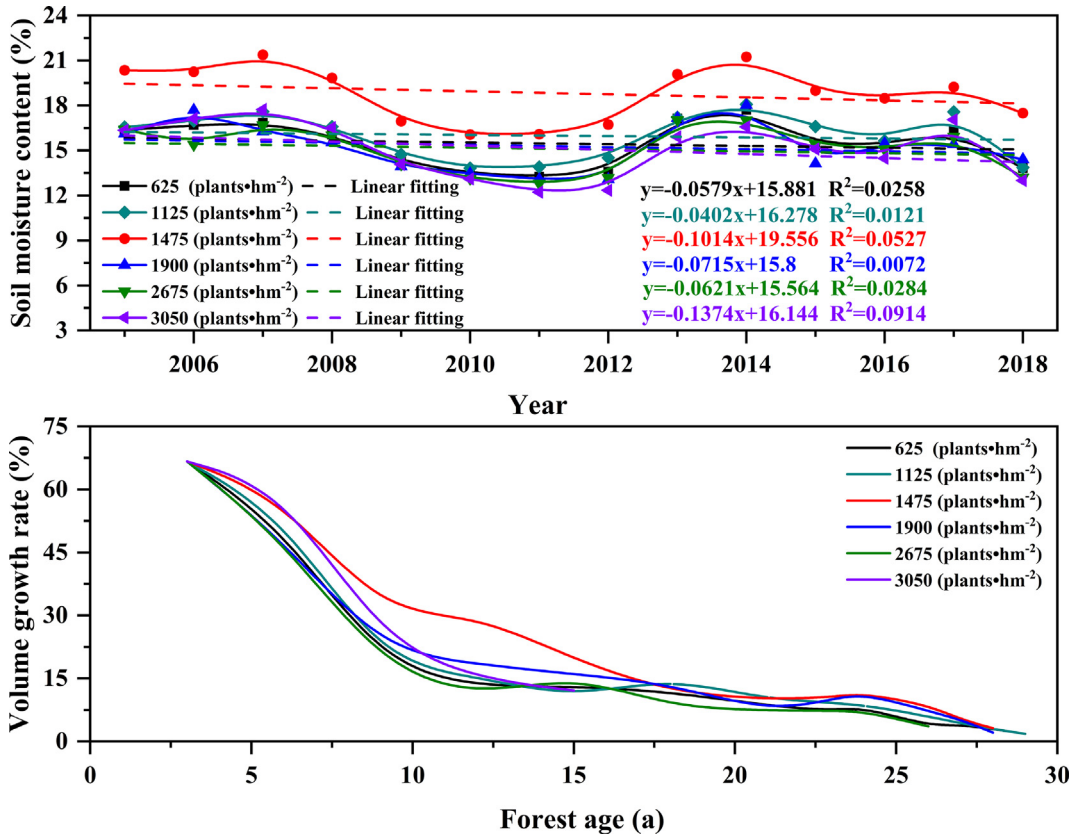

Fig. 6. The change trends of the soil moisture content and volume growth rate of wood during vegetation restoration.

vegetation restoration are shown in Fig. 6. The SMC and the volume growth rate of *R. pseudoacacia* forests presented a declining trend during vegetation restoration overall. Both the SMC and volume growth rate of *R. pseudoacacia* forestland (1475 plants·hm^{-2}) were higher than those of the other *R. pseudoacacia* forestlands. The volume growth rate of *R. pseudoacacia* forest growth was slow after 10 s, i.e., forests growth increased slowly after 10 s, and the volume growth rate of the *R. pseudoacacia* forests was less than 10%. There are two possible reasons for this result—one is that *R. pseudoacacia* forests start aging slowly, and the other is that the growth of *R. pseudoacacia* forests is limited by the soil moisture.

3.2.3. Influence of stand structure on the low-efficiency level of the R. pseudoacacia forest

It is important to formulate a set of highly targeted and efficient optimization technologies for the optimization of stand structure considering the four stand growth conditions of the *R. pseudoacacia* forest. Therefore, the relationships of stand structure and the SWBI models of the four stand growth statuses were constructed. Fig. 7 indicates that the *P* values of all four models were greater than 0.05 (0.101, 0.095, 0.121 and 0.145), and the stable coefficients of these four models were 0.88, 0.99, 0.97 and 0.98, respectively, indicating that models I, II, III and IV were not rejected and could well reflect the relationship between the stand structure and the soil and water conservation ecological benefits of the four different growth statuses of *R. pseudoacacia* forests. Model I showed that the SD, CA, TCI and LAI had significant effects on the soil and water conservation ecological benefits for the healthy type of forest. Model II indicated that the SD, TH, CA and LAI had significant effects on the soil and water conservation ecological benefits for forests with a mild level of low efficiency. Model III suggested that the SD, CD, TH, TCI and AS had significant effects on the soil and water conservation ecological benefits in forests with a moderate level of low efficiency, while model IV implied that the SD, CD, TH, TCI and LAI had significant effects on the soil and water conservation ecological benefits in forests with a severe level of low efficiency. Additionally, the four structural and functional models all showed that SD had a great influence on other stand structure index factors. Therefore, the method of improving the soil and water conservation ecological benefits by optimizing the SD factor and then optimizing other stand structure indicators provides ideal theoretical guidance for optimization.

3.3. Optimization of stand structures of low-efficiency R. pseudoacacia forest

3.3.1. Characteristics of the main stand structures of the R. pseudoacacia forest

The SD was mainly between 1400 and 1600 plants·hm^{-2} in the healthy forest type, and the CD, LAI, TCI, TH and CA mainly ranged from 0.61–0.67, 2.05–2.35, 1.94–2.16, 9–10 m and 7–8 m^2, respectively (Fig. 8). The SD ranged mainly between ~1200 and ~2400 plants·hm^{-2} in the forest with a mild level of low efficiency, and the CD, LAI, TCI, TH and CA mainly ranged between ~0.59 and ~0.67, ~1.5 and ~ 2.5, ~1.7 and ~2.3, ~8.4 m, and ~6.7 m^2 and ~8.2 m^2, respectively. However, the SD mainly ranged between ~750 and ~2750 plants·hm^{-2}, in forests with a moderate level of low efficiency, and the CD, LAI, TCI, TH and CA mainly ranged between ~0.53 and ~0.77, ~1.25 and ~2.75, ~1.5 and ~2.7, ~6.9 m, and ~5 m^2 and ~11 m^2, respectively. In the forest with a severe level of low efficiency, the SD mainly ranged between 450 and ~3250 plants·hm^{-2}, and the CD, LAI, TCI, TH and CA mainly ranged between ~0.4 and ~0.6, ~0.5 and ~4.5, ~1.35 and ~4.1, ~4.4 m and ~6 m, and ~2 m^2 and ~16 m^2, respectively.

Additionally, Table 6 suggests a better-fitting effect of the Weibull and gamma distributions for stand structure in the healthy type of forest, as determined through K-S testing. In comparison to the other three density functions, the gamma and lognormal distributions showed

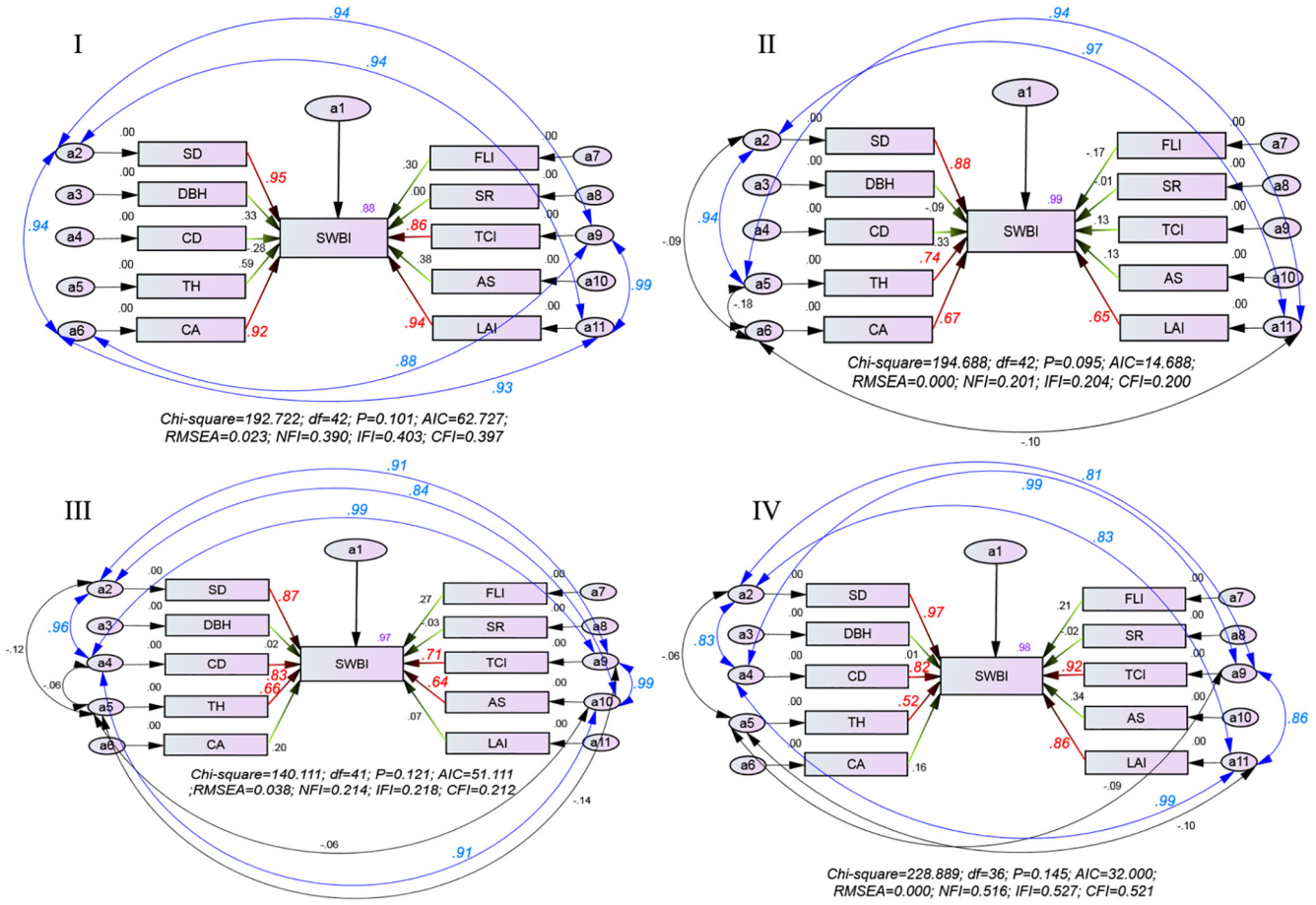

Fig. 7. Relationships between the stand structure and the SWBI for the no/mild/moderate/severe levels of low efficiency in *R. pseudoacacia* forests.

a better-fitting effect through K-S testing on stand structure in the *R. pseudoacacia* forests with mild and moderate levels of low efficiency. However, the exponential distribution showed a better-fitting effect for stand structure in the *R. pseudoacacia* forest with a severe level of low efficiency.

3.3.2. Optimal results for the stand structure of low-efficiency R. pseudoacacia forests

The RSM results of the three status levels (mild, moderate and severe) of the low-efficiency forests are shown in Figs. 9 to 11. The R^2 of these three quadratic multiple regression equations was more than 0.9, the predicted R^2 was reasonably consistent with the adjusted R^2, and all *P* values were less than 0.05, which indicated that the quadratic multiple regression equations were significant. Additionally, adequate precision further indicated that these three quadratic multiple regression equations could be used to determine the optimization of the stand structures of the *R. pseudoacacia* forest with mild, moderate and severe levels of low efficiency.

The RSM predicted that the optimal stand structure configuration in the forest with a mild level of low efficiency was SD = 1698, TH = 11, CA = 7.52, and LAI = 2.35; according to the prediction, the SWBI was 9.31798, and in comparison to the average SWBI (5.00), it was expected to improve by approximately 86%. The optimal stand structure configuration in the forest with a moderate level of low efficiency was SD = 1529, CD = 0.66, TH = 9.86, TCI = 2.14, and AS = 0.62, and in comparison to the average SWBI (3.19), the predicted SWBI (9.57074) was expected to improve approximately 2 times more. The optimal stand structure configuration in the forest with a severe level of low efficiency was SD = 1459, CD = 0.61, TH = 9.39, TCI = 2.03, and LAI = 2.13, and in comparison to the SWBI (1.18) before optimization, the SWBI was expected to improve approximately 6 times more.

4. Discussion

4.1. Effects of stand density and leaf area index on low-efficiency levels of the R. pseudoacacia forest

The Loess Plateau is an area with minimal vegetation coverage, making soil erosion in the area a serious problem (Wei et al., 2010). The main objective of afforestation projects is to increase vegetation coverage to reinforce soil and water conservation in arid and semiarid areas (Fu et al., 2011). Therefore, increasing SD is a simple and feasible measure to achieve this objective. Forest ecosystems contain numerous individual trees. SD is a key stand structural factor that plays an important role during vegetation succession (Sizemskaya et al., 2009; Deng et al., 2016; Nan et al., 2019). The results of this study suggested that an SD value over the low level (~500 plants·hm^{-2}) or over the high level (~3000 plants·hm^{-2}) and an LAI value over the low level (less than 1) or over the high level (more than 5) will result in low levels of soil and water conservation ecological benefits from the *R. pseudoacacia* forest (Fig. 3). From the perspective of forest hydrology, there are two main reasons for this distribution characteristic.

First, the amount of soil moisture inputs is declining in *R. pseudoacacia* forests, and the growth of *R. pseudoacacia* forests is slowing (Fig. 6). This result is similar to the results of Wang et al. (2016) and Liang et al. (2018). Water is the main factor affecting the survival and growth of vegetation (Kurc and Benton, 2010; Zhang et al., 2018a). Precipitation is the main resource of soil moisture supplementation (Jia et al., 2019). The results of this study suggest that precipitation declined at a rate of 0.52 mm/a from 1957 to 2018 (Fig. 4), although this

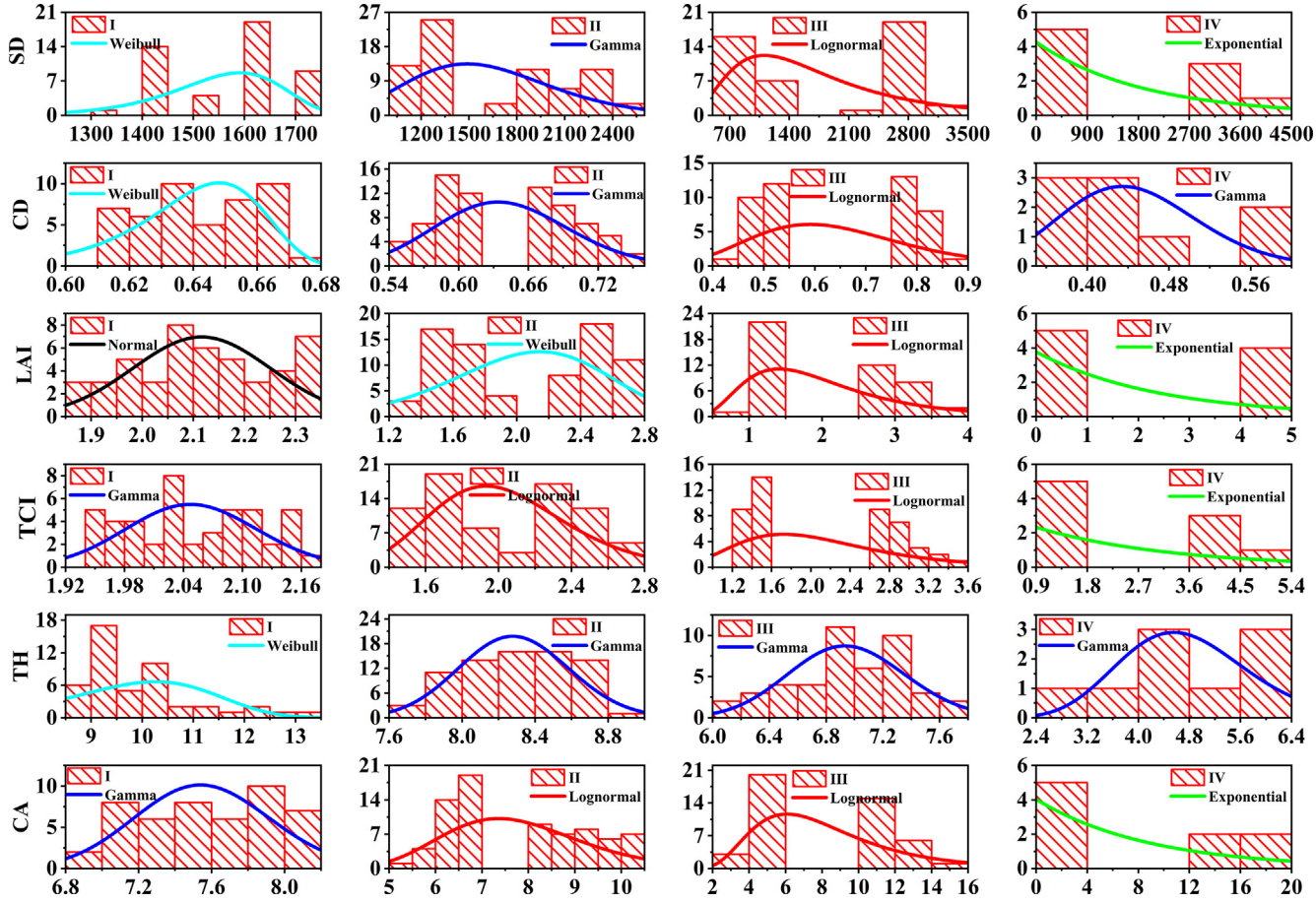

Fig. 8. Distribution characteristics of the main stand structure of the *R. pseudoacacia* forests with no/mild/moderate/severe levels of low efficiency.

Table 6
Parameters and test results of the SD/CD/CATCI/TH/LAI distribution models of the efficiency of the *R. pseudoacacia* forest.

Indicators	Types	Distribution model	Para	Value		Testing (K-S)
SD	I	Weibull	γ, β	1597.54	16.00	0.059
	II	Gamma	α, β	12.42	130.39	0.052
	III	Lognormal	μ, σ	7.33	0.57	0.058
	IV	Exponential	λ	1900.00	/	0.153
CD	I	Weibull	γ, β	0.65	37.87	0.096
	II	Gamma	α, β	126.42	91.83	0.193
	III	Lognormal	μ, σ	−0.47	0.24	0.152
	IV	Gamma	α, β	44.06	0.01	0.248
CA	I	Normal	μ, σ	7.55	0.37	0.151
	II	Weibull	γ, β	8.43	5.73	0.123
	III	Lognormal	μ, σ	2.01	0.46	0.147
	IV	Exponential	λ	8.93	/	0.158
TCI	I	Gamma	α, β	941.28	0.01	0.086
	II	Lognormal	μ, σ	0.69	0.19	0.143
	III	Lognormal	μ, σ	0.69	0.38	0.128
	IV	Exponential	λ	2.38	/	0.152
TH	I	Weibull	γ, β	10.43	7.96	0.083
	II	Gamma	α, β	751.03	0.01	0.256
	III	Gamma	α, β	285.05	0.02	0.257
	IV	Gamma	α, β	22.34	0.21	0.258
LAI	I	Gamma	α, β	250.47	0.01	0.253
	II	Lognormal	μ, σ	0.69	0.24	0.122
	III	Lognormal	μ, σ	0.60	0.51	0.126
	IV	Exponential	λ	2.39	/	0.156

trend was not significant. These results indicate that the main source of soil moisture supplementation is gradually decreasing. Therefore, from the perspective of SMC supplementation, the SMC is declining. These results are similar to the results of Zhao et al. (2017) and Zhang et al. (2018b). Their results indicated that the Loess Plateau is currently associated with a drought trend and that the drought degree will likely continue to increase. These conclusions have been validated in this study (Fig. 4, Fig. 5 and Table 5). Therefore, the SMC of the *R. pseudoacacia* forests will certainly decrease with climate change. The SD and LAI that are higher than the low levels may cause runoff loss, and SMC cannot be supplemented with effective precipitation (Jia et al., 2017a). However, the SD and LAI that are higher than the high levels also result in precipitation that is intercepted by the canopy layer, and SMC cannot be supplemented (Jian et al., 2015; Jia et al., 2019). Therefore, the SD, LAI and CA have significant effects on the SWBI regardless of the low efficiency level of the *R. pseudoacacia* forests used in this study (Fig. 7). This result is similar to the results of Chen et al. (2007).

Second, the amount of soil moisture outputs is increasing in *R. pseudoacacia* forests. The results of linear trend estimation in this study suggested that the air temperature increased at a rate of 0.227 °C/10a from 1957 to 2018 (Fig. 4), and this increasing trend of the air temperature is significant both seasonally and annually (Table 5). This change trend is similar to the results of Wang et al. (2011) and Zhao et al. (2017). This change trend can result in an increase in the soil evaporation rate and the vegetation transpiration rate and gradually accelerate the consumption of soil moisture (Jian et al., 2015). Hou et al. (2019) reported that the vegetation transpiration rate in the *R. pseudoacacia* forest was 0.91 ± 0.02 $mm{\cdot}L^{-1}$, which greatly accelerated the rates of soil water consumption and forestland degradation. Liu et al. (2019) applied hydrogen and oxygen isotopes (δ^2H and $\delta^{18}O$) to demonstrate that plants mainly use soil moisture in maintaining plant activities, and they reported the important finding that plants absorb soil moisture in the topsoil layer when water resources

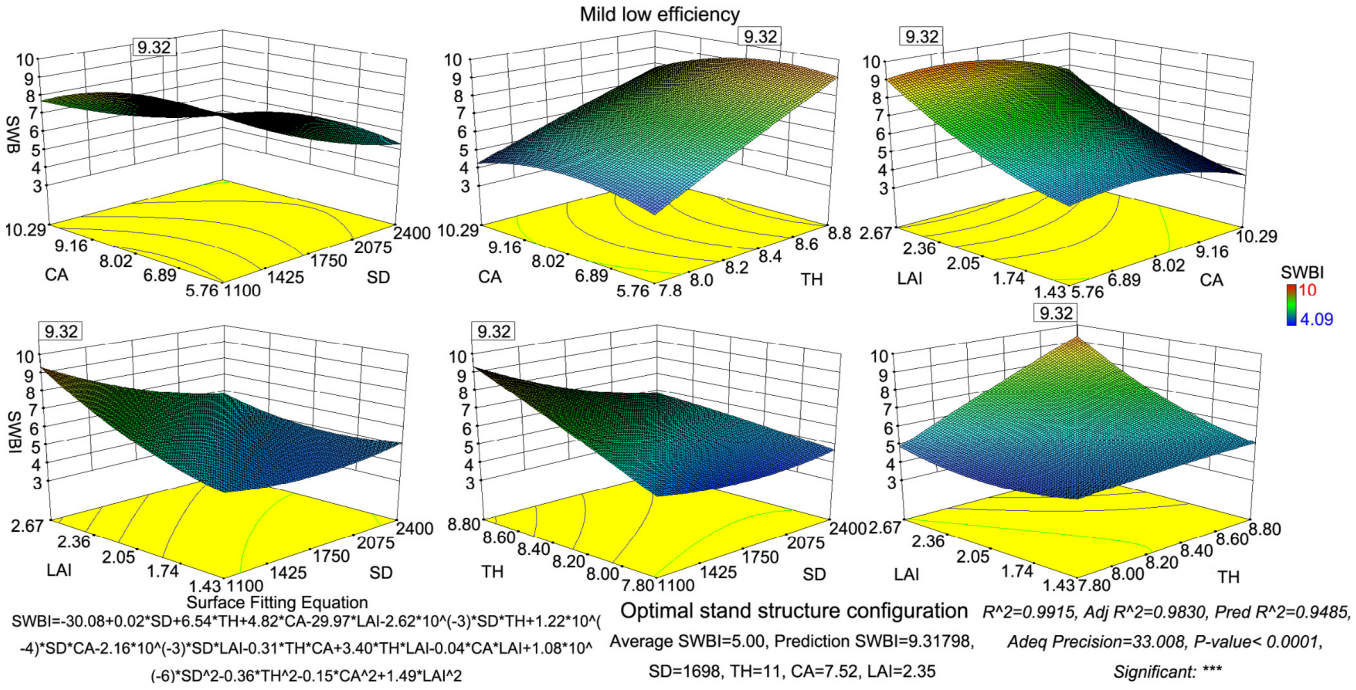

Fig. 9. Optimal results of the stand structure in the *R. pseudoacacia* forest with a mild level of low efficiency.

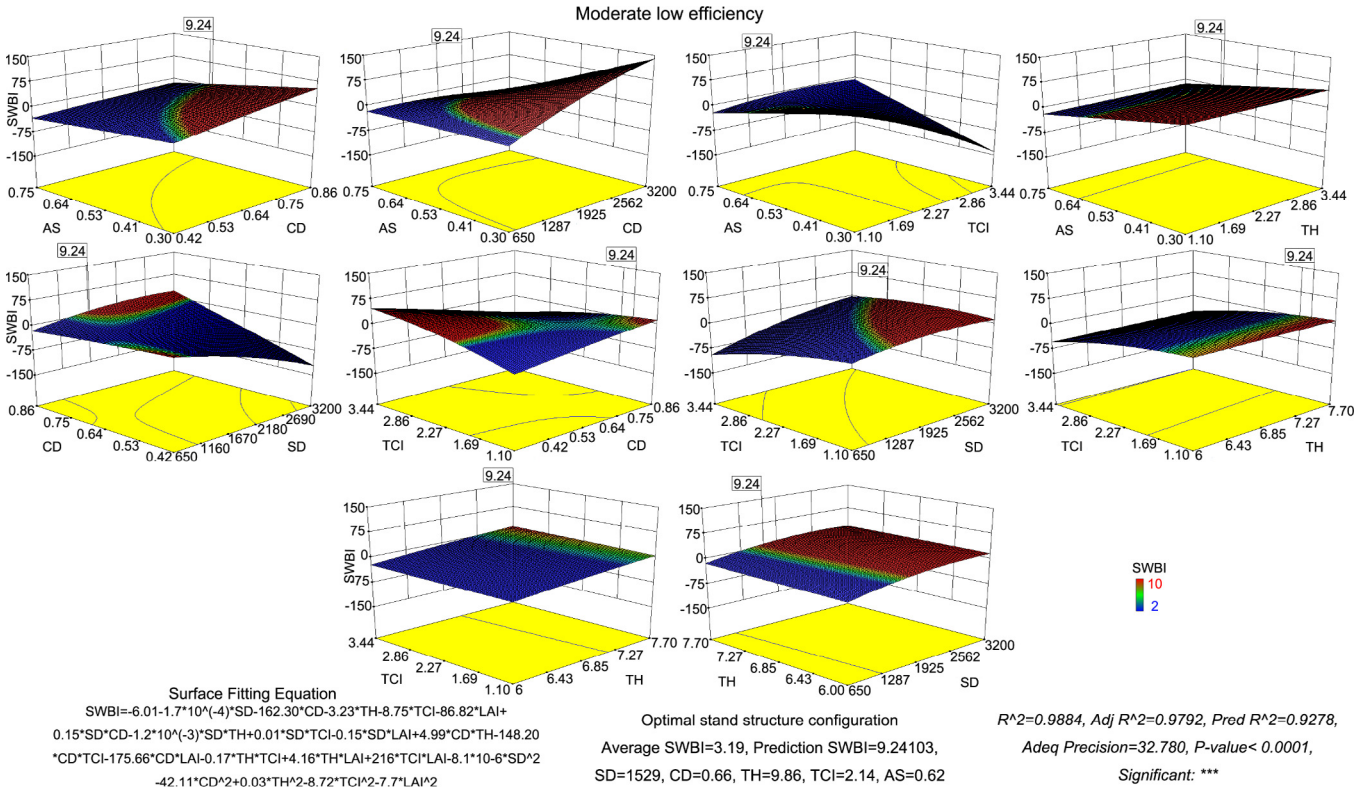

Fig. 10. Optimal results of the stand structure in the *R. pseudoacacia* forest with a moderate level of low efficiency.

are sufficient; however, water uptake is switched to deeper soil layers once the soil moisture in the topsoil layer is deficient. Additionally, Cao et al. (2009) also reported that in comparison to natural grass and crops, woody species could consume more soil water via evapotranspiration. Soils become extremely dry in both deep and shallow layers after trees are planted (Wang et al., 2010; Jia and Shao, 2014). A change in air temperature can also result in an increase in the soil evaporation rate and the vegetation transpiration rate and gradually accelerate the consumption of soil moisture, resulting in soil desiccation and dry soil layer formation. Therefore, SD should be controlled at ~1500 plants·hm^{-2}, and the LAI should be controlled at ~2.5 in low-efficiency *R. pseudoacacia* forests to maintain the balance of soil moisture inputs and outputs. These results are similar to the results of Bi et al. (2007) and Chi et al. (2018).

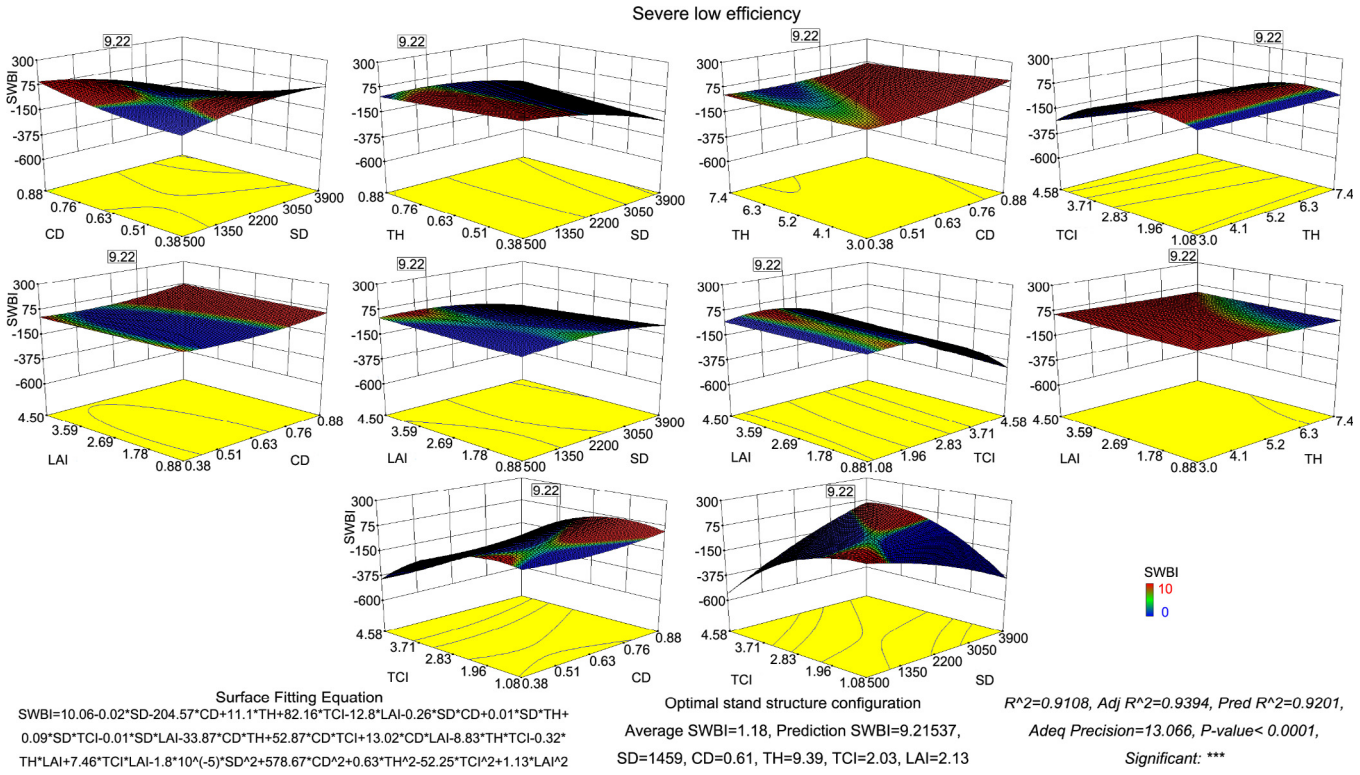

Fig. 11. Optimal results of the stand structure in the *R. pseudoacacia* forest with a severe level of low efficiency.

4.2. Optimal stand structures for the low-efficiency R. pseudoacacia forest

The optimization of stand structures in low-efficiency *R. pseudoacacia* forest is the most important objective of this study. Optimizing the stand structure of low-efficiency *R. pseudoacacia* forests requires referencing healthy forests (Diemont et al., 2011; Chen et al., 2015; Wang et al., 2018; Mo et al., 2016). Understanding the characteristics of the stand structure of every forest type is helpful in determining the optimization objective of main stand structure indicators (Carlos et al., 2016; Zhang et al., 2018a). Fig. 6 shows the same change trend for the six indicators (SD, CD, LAI, TCI, TH and CA) where the value appeared polarized in forests with mild, moderate and severe levels of low efficiency, and this phenomenon was more obvious with increasing degrees of low-efficiency. This change indicated that the values of these six indicators that were greater than high or low levels would cause the low-efficiency levels of *R. pseudoacacia*. This result is similar to the results of Jia et al. (2019) and Zhang et al. (2017).

The optimal configuration of the stand structures in *R. pseudoacacia* forests with mild/moderate/severe levels of low efficiency was affected differently when climate change presented the same trend; therefore, the optimal stand structures were different in the low-efficiency *R. pseudoacacia* forest (Fig. 9 to Fig. 11). There are some reasons to explain this result. The main and important reason for this result is the different underlying surface conditions. The slope, SD and LAI were different (Table 1), which affected the soil and vegetation characteristics. In addition, the underlying surface conditions (soil moisture, soil nutrients, soil physical properties, root distribution, and structures of understory shrubs and herbs as well as litter) are affected differently by initial SDs and by the varied stand characteristics during the process of revegetation (Jia et al., 2017a, b; Zhang et al., 2017). In this study, CA, CD, TH, FLI, angle scale and LAI were very different in the *R. pseudoacacia* forest with mild/moderate/severe levels of low efficiency. These stand indicators affect soil moisture supplementation by changing the form and intensity of rainfall and indirectly affect the transport of soil nutrients (N, P, and K) (Jia et al., 2005; Zhao et al., 2010; Zhang et al., 2016). The controllable degrees of stand improvement in these three low-efficiency *R. pseudoacacia* forests were also different, which resulted in the optimal configurations of the stand structures the *R. pseudoacacia* forest with mild/moderate/severe levels of low efficiency being different. Additionally, the results in Table 4 and Fig. 6 and Fig. 8 validated that when the SD of a *R. pseudoacacia* forest is controlled to approximately 1500 plants·hm^{-2}, the soil and water conservation ecological benefits are better (SWBI $>$ 6). Therefore, the application of the conclusions in Fig. 9, Fig. 10 and Fig. 11 to optimize the disposition of stand structures of low-efficiency of *R. pseudoacacia* forest is reasonable and practicable. The three hypotheses presented in the introduction have been validated based on the analytical results in this study.

5. Conclusion

This paper systematically proposed a more complete process for optimizing the stand structure of a *R. pseudoacacia* forest at different levels of low efficiency based on a comprehensive index of soil and water conservation ecological benefits. This study demonstrated that the soil and water conservation ecological benefits of the *R. pseudoacacia* forest will present low efficiency levels with threatening effects because improper stand structures and changes in water resources occur as the number of recovery years increases. The low-efficiency *R. pseudoacacia* forest was divided into three levels of low efficiency, mild, moderate and severe, based on the SWBI. The functions of Weibull, lognormal and exponential can better fit the distribution characteristics of stand structure in *R. pseudoacacia* forests with mild, moderate and severe levels of low efficiency, respectively. The optimal stand structure configurations are SD = 1698, TH = 11, CA = 7.52, and LAI = 2.35 in a forest with a mild level of low efficiency; SD = 1529, CD = 0.66, TH = 9.86, TCI = 2.14, and AS = 0.62 in a forest with a moderate level of low efficiency; and SD = 1459, CD = 0.61, TH = 9.39, TCI = 2.03, and LAI = 2.13 in a forest with a severe level of low efficiency. Additionally, planting *R. pseudoacacia* forests was not an

incorrect choice, but the stand structures need to be optimized to maintain the ecological balance in arid and semiarid regions. It is suggested that the optimization of the stand structures of low-efficiency forests on the Loess Plateau in China should be carried out in stages to prevent the deterioration of ecological benefits caused by one-time stand structure adjustments.

Declaration of Competing Interest

The authors declare that they have no known competing financial interests or personal relationships that could have appeared to influence the work reported in this paper.

Acknowledgments

This research was supported by the National Natural Science Funds of China (No. 31971725), the National Key Research and Development Program of China (No. 2016YFC0501704) and the Beijing Collaborative Innovation Center for Eco-environmental Improvement with Forestry and Fruit Trees (PXM2019_014207_000024). We would like to thank the anonymous reviewers and the editor and associate editor for the thorough assessment of this paper and for the many valuable and helpful suggestions.

Author contributions

Guirong Hou and Huaxing Bi conceived the paper; Guirong Hou wrote and revised the paper; Huaxing Bi provided constructive suggestions; Guirong Hou, Xi Wei, Ning Wang, Yanhong Cui, Danyang Zhao, Xiaozhi Ma, and Shanshan Wang conducted the forest investigations and experiments.

References

Ahmad, B., Wang, Y.H., Hao, J., Liu, Y.H., Bohnett, E., Zhang, K.B., 2018. Optimizing stand structure for trade-offs between overstory timber production and understory plant diversity: a case-study of a larch plantation in northwest China. Land Degrad. Dev. 29, 2998–3008. https://doi.org/10.1002/ldr.3070.

Bi, H.X., Li, X.Y., Li, J., Guo, M.X., Liu, X., 2007. Study on suitable vegetation cover on Loess Area based on soil water balance. Sci. Ailvae Ainicae 43 (4), 17–23. https://doi.org/10.11707/j.1001-7488.20070403.

Cao, S.X., Chen, L., Yu, X.X., 2009. Impact of China's Grain for Green Project on the landscape of vulnerable arid and semi-arid agricultural regions: a case study in northern Shaanxi Province. J. Appl. Ecol. 46, 536–543. https://doi.org/10.1111/j.1365-2664.2008.01605.x.

Carlos, V.P., Fernando, C.L., Gilberto, V.L., Noel, G.V., Iván, O.O., Víctor, D.E., 2016. Influence of the density of scattered trees in pastures on the structure and species composition of tree and grass cover in southern Tabasco, Mexico. Agric. Ecosyst. Environ. 232, 1–8. https://doi.org/10.1016/j.agee.2016.07.020.

Chen, L.D., Huang, Z.L., Gong, J., Fu, B.J., Huang, Y.L., 2007. The effect of land cover/vegetation on soil water dynamic in the hilly area of the loess plateau, China. Catena 70, 200–208. https://doi.org/10.1016/j.catena.2006.08.007.

Chen, Y.P., Wang, K.B., Lin, Y.S., Shi, W.Y., Song, Y., He, X.H., 2015. Balancing green and grain trade. Nat. Geosci. 8, 739–741. https://doi.org/10.1038/ngeo2544.

Cheng, G.D., Li, X., Zhao, W.Z., Xu, Z.M., Feng, Q., Xiao, S.C., Xiao, H.L., 2014. Integrated study of the water-ecosystem-economy in the Heihe River Basin. Natl. Sci. Rev. 1, 413–428. https://doi.org/10.1093/nsr/nwu017.

Chi, D.K., Wang, H., Li, X.B., Liu, H.H., Li, X.H., 2018. Estimation of the ecological water requirement for natural vegetation in the Ergune River basin in Northeastern China from 2001 to 2014. Ecol. Indic. 92, 141–150. https://doi.org/10.1016/j.ecolind.2017.04.014.

Deng, L., ShangGuan, Z.P., Li, R., 2012. Effects of the grain-for-green program on soil erosion in China. Int. J. Sediment Res. 27, 120–127. https://doi.org/10.1016/S1001-6279(12)60021-3.

Deng, L., Yan, W.M., Zhang, Y.W., Shangguan, Z.P., 2016. Severe depletion of soil moisture following land-use changes for ecological restoration: evidence from northern China. For. Ecol. Manage. 366, 1–10. https://doi.org/10.1016/j.foreco.2016.01.026.

Duan, L.X., Huang, M.B., Li, Z.W., Zhang, Z.D., Zhang, L.D., 2017. Estimation of spatial mean soil water storage using temporal stability at the hillslope scale in black locust (*Robinia pseudoacacia*) stands. Catena 156, 51–61. https://doi.org/10.1016/j.catena.2017.03.023.

Diemont, S.A.W., Bohn, J.L., Rayome, D.D., Kelsen, S.J., Cheng, K.T., 2011. Comparisons of Mayan forest management, restoration, and conservation. Forest Ecol. Manage. 261, 1696–1705. https://doi.org/10.1016/j.foreco.2010.11.006.

Fu, B.J., Liu, Y., Lü, Y.H., He, C.S., Zeng, Y., Wu, B.F., 2011. Assessing the soil erosion control service of ecosystems change in the Loess Plateau of China. Ecol. Complex 8, 284–293. https://doi.org/10.1016/j.ecocom.2011.07.003.

Gao, X.D., Wu, P.T., Zhao, X.N., Wang, J.W., Shi, Y.G., Zhang, B.Q., Tian, L., Li, H.B., 2013. Estimation of spatial soil moisture averages in a large gully of the Loess Plateau of China through statistical and modeling solutions. J. Hydrol. 486, 466–478. https://doi.org/10.1016/j.jhydrol.2013.02.026.

García-Ruiz, J.M., 2010. The effects of land uses on soil erosion in Spain: a review. Catena 81, 1–11. https://doi.org/10.1016/j.catena.2010.01.001.

Hou, G.R., Bi, H.X., Wang, N., Cui, Y.H., Ma, X.Z., Zhao, D.Y., Wang, S.S., 2019. Optimizing the stand density of low-efficiency *Robinia pseudoacacia* forests of the Loess Plateau, China, based on the response relationship of stand density to soil water and soil nutrient resources. Forests 10 (8), 663. https://doi.org/10.3390/f10080663.

Hui, G.Y., Klaus, V.G., Hu, Y.B., Xu, H., 2007. Structure-based forest management, Beijing.

Jia, G.M., Cao, J., Wang, C.Y., Wang, G., 2005. Microbial biomass and nutrients in soil at the different stages of secondary forest succession in Ziwulin, northwest China. For. Ecol. Manage. 217, 117–125. https://doi.org/10.1016/j.foreco.2005.05.055.

Jia, X.X., Shao, M.A., Yu, D.X., Zhang, Y., Andrew, Binley, 2019. Spatial variations in soil-water carrying capacity of three typical revegetation species on the Loess Plateau, China. Agric. Ecosyst. Environ. 273, 25–35. https://doi.org/10.1016/j.agee.2018.12.008.

Jia, X.X., Shao, M.A., Zhu, Y.J., Luo, Y., 2017a. Soil moisture decline due to afforestation across the Loess Plateau, China. J. Hydrol. 546, 113–122. https://doi.org/10.1016/j.jhydrol.2017.01.011.

Jia, X.X., Wang, Y.Q., Shao, M.A., Luo, Y., Zhang, C.C., 2017b. Estimating regional losses of soil water due to the conversion of agricultural land to forest in China's Loess Plateau. Ecohydrology. 10 (6), e1851. https://doi.org/10.1002/eco.1851.

Jia, Y.H., Shao, M.A., 2014. Dynamics of deep soil moisture in response to vegetational restoration on the Loess Plateau of China. J. Hydrol. 519, 523–531. https://doi.org/10.1016/j.jhydrol.2014.07.043.

Jian, S.Q., Zhao, C.Y., Fang, S.M., Yu, K., 2015. Effects of different vegetation restoration on soil water storage and water balance in the Chinese Loess Plateau. Agric. Forest Meteo. 206, 85–96. https://doi.org/10.1016/j.agrformet.2015.03.009.

Jiang, X.J., Liu, W.J., Wu, J.N., Wang, P.Y., Liu, C.G., Yuan, Z.Q., 2017. Land degradation controlled and mitigated by rubber-based agroforestry systems through optimizing soil physical conditions and water supply mechanisms: a case study in XiShuangBanna, China. Land Degrad. Dev. 28, 2277–2289. https://doi.org/10.1002/ldr.2757.

Kurc, S., Benton, L., 2010. Digital image-derived greenness links deep soil moisture to carbon uptake in a creosotebush-dominated shrubland. J. Arid Environ. 74, 585–594. https://doi.org/10.1016/j.jaridenv.2009.10.003.

Li, F.R., Zhao, A.F., Zhou, H.Y., Zhang, T.H., Zhao, X., 2002. Effects of simulated grazing on growth and persistence of Artemisia frigida in a semiarid sandy rangeland. Grass Forage Sci. 57, 239–246. https://doi.org/10.1046/j.1365-2494.2002.00322.x.

Li, Y.F., Hui, G.Y., Zhao, Z.H., Hu, Y.B., 2012. The bivariate distribution characteristics of spatial structure in natural Korean pine broad-leaved forest. J. Veg. Sci. 23, 1180–1190. https://doi.org/10.1111/j.1654-1103.2012.01431.x.

Liang, H.B., Xue, Y.Y., Li, Z.S., Wang, S., Wu, X., Gao, G.Y., Liu, G.H., Fu, B.J., 2018. Soil moisture decline following the plantation of *Robinia pseudoacacia* forests: evidence from the Loess Plateau. Forest Ecol. Manage. 412, 62–69. https://doi.org/10.1016/j.foreco.2018.01.041.

Liu, Z.Q., Yu, X.X., Jia, G.D., 2019. Water uptake by coniferous and broad-leaved forest in a rocky mountainous area of northern China. Agric. Forest Meteorol. 265, 381–389. https://doi.org/10.1016/j.agrformet.2018.11.036.

Liu, Z.Q., Yu, X.X., Jia, G.D., 2020. Variation of water uptake in degradation agroforestry shelterbelts on the North China Plain. Agric. Ecosyst. Environ. 287, 106697. https://doi.org/10.1016/j.agee.2019.106697.

Ludwig, J.A., Wilcox, B.P., Breshears, D.D., Tongway, D.J., Imeson, A.C., 2005. Vegetation patches and runoff-erosion as interacting ecohydrological processes in semiarid landscapes. Ecology 86, 288–297. https://doi.org/10.1890/03-0569.

Ma, C., Wang, Y.J., Du, C., Wang, Y.Q., Li, Y.P., 2016. Variation in initiation condition of debris flows in the mountain regions surrounding Beijing. Geomorphology 273, 323–334. https://doi.org/10.1016/j.geomorph.2016.08.027.

Ma, C., Wang, Y.J., Hu, K.H., Du, C., Yang, W.T., 2017. Rainfall intensity-duration threshold and erosion competence of debris flows in four areas affected by the 2008 Wenchuan earthquake. Geomorphology 282, 85–95. https://doi.org/10.1016/j.geomorph.2017.01.012.

Meng, K., Garcia-Fayos, P., Hu, S., Jiao, J.Y., 2016. The effect of *Robinia pseudoacacia* afforestation on soil and vegetation properties in the Loess Plateau (China): a chronosequence approach. Forest Ecol. Manage. 375, 146–158. https://doi.org/10.1016/j.foreco.2016.05.025.

Mo, K.L., Cong, Z.T., Lei, H.M., 2016. Optimal vegetation cover in the Horqin Sands, China. Ecohydrology 9, 700–711. https://doi.org/10.1002/eco.1668.

Nan, G.W., Wang, N., Jiao, L., Zhu, Y.M., Sun, H., 2019. A new exploration for accurately quantifying the effect of afforestation on soil moisture: a case study of artificial *Robinia pseudoacacia* in the Loess Plateau (China). For. Ecol. Manage. 433, 459–466. https://doi.org/10.1016/j.foreco.2018.10.029.

Ouyang, Z.H., Zheng, H., Xiao, Y., Polasky, S.P., Liu, J.G., Xu, W.H., Wang, Q., Zhang, L., Xia, Y., 2016. Improvements in ecosystem services from investments in natural capital. Science 352, 1455–1459. https://doi.org/10.1126/science.aaf2295.

Singh, A., Shi, H., Foresman, T., Fosnight, E.A., 2001. Status of the world's remaining closed forests: an assessment using satellite data and policy options. Ambio J. Hum. Environ. 30, 67–69. https://doi.org/10.1579/0044-7447-30.1.67.

Sizemskaya, M.L., Jiao, J.Y., Wang, N., Sapanov, M.K., Wu, Q.X., Jia, Y.F., Kolesnikov, A.V., Liu, G.B., Sapanov, P.M., 2009. Specificity of afforestation under conditions of

moisture deficit in south of Russian plain and the Loess Plateau of China. Res. Soil Water Conserv. 16, 73–77. https://doi.org/10.1007/978-1-4020-9623-5_5.

Pukkala, T.M., LähdeM, E., Laiho, Olavi, 2010. Optimizing the structure and management of uneven-sized stands of Finland. Forestry 83, 2. https://doi.org/10.1093/forestry/cpp037.

Vítková, M., Müllerová, J., Sádlo, J., Pergl, J., Pyšek, P., 2017. Black locust (*Robinia pseudoacacia*) beloved and despised: a story of an invasive tree in Central Europe. Forest Ecol. Manage. 384, 287–302. https://doi.org/10.1016/j.foreco.2016.10.057.

Wang, H.J., Zhou, H., 2003. A simulation study on the eco-environmental effects of 3N Shelterbelt in North China. Global Planet. Change 37, 231–246. https://doi.org/10.1016/S0921-8181(02)00208-4.

Wang, Y.H., Xiong, W., Gampe, S., Coles, N.A., Yu, P.T., Xu, L.H., Zuo, H.J., Wang, Y.N., 2015. A water yield-oriented practical approach for multifunctional forest management and its application in dryland regions of China. J. Am. Water Resour. Assoc. 51, 689–703. https://doi.org/10.1111/1752-1688.12314.

Wang, Y., Zhu, Q.K., Zhao, W.J., Ma, H., Wang, R., Ai, N., 2016. The dynamic trend of soil water content in artificial forests on the Loess Plateau, China. Forests 7, 236. https://doi.org/10.3390/f7100236.

Wang, Y.H., Yu, P.T., Wang, J.Z., Xu, L.H., Feger, K.H., Xiong, W., 2017. Multifunctional Forestry on the Loess Plateau. Multifunctional Land-use Systems for Managing the Nexus of Environmental Resources. Springer, pp. 79–107.

Wang, Y.Q., Shao, M.A., Shao, H.B., 2010. A preliminary investigation of the dynamic characteristics of dried soil layers in the Loess Plateau of China. J. Hydrol. 381, 9–17. https://doi.org/10.1016/j.jhydrol.2009.09.042.

Wang, Y.Q., Shao, M.A., Zhu, Y.J., Liu, Z.P., 2011. Impacts of land use and plant characteristics on dried soil layers in different climatic regions on the Loess Plateau of China. Agric. Forest Meteorol. 151, 437–448. https://doi.org/10.1016/j.agrformet.2010.11.016.

Wei, W., Chen, L.D., Fu, B.J., Chen, J., 2010. Water erosion response to rainfall and land use in different drought-level years in a loess hilly area of China. Catena 8, 24–31. https://doi.org/10.1016/j.catena.2010.01.002.

Wei, X., Bi, H.X., Liang, W.J., Hou, G.R., Kong, L.X., Zhou, Q.Z., 2018. Relationship between soil characteristics and stand structure of *Robinia pseudoacacia* L. and *Pinus tabulaeformis* Carr. mixed plantations in the Caijiachuan watershed: an application of structural equation modeling. Forests 9, 124. https://doi.org/10.3390/f9030124.

Wang, S., Fu, B.J., Chen, H.B., Liu, Y., 2018. Regional development boundary of China's Loess Plateau: water limit and land shortage. Land Use Policy 6, 1019–1022. https://doi.org/10.1016/j.landusepol.2017.03.003.

Xin, Z.B., Yu, B.F., Han, Y.G., 2015. Spatiotemporal variations in annual sediment yield from the middle yellow river, China, 1950–2010. J. Hydrol. Eng. 20, 04014090. https://doi.org/10.1061/(ASCE)HE.1943-5584.0001113.

Zhang, K.C., An, Z.S., Cai, D.W., Guo, Z.C., Xiao, J.H., 2017. Key role of desert-oasis transitional area in avoiding oasis land degradation from aeolian desertification in Dunhuang, Northwest China. Land Degrad. Dev. 28, 142–150. https://doi.org/10.1002/ldr.2584.

Zhang, S.L., Yang, D.W., Yang, Y.T., Piao, S.L., Yang, H.B., Lei, H.M., Fu, B.J., 2018a. Excessive afforestation and soil drying on China's Loess Plateau. J. Geophys. Res.-Biogeo. 123, 923–935. https://doi.org/10.1002/2017JG004038.

Zhang, Y.K., Huang, M.B., Hu, W., Suo, L.Z., Duan, L.X., Wu, L.H., 2018b. How shallow and how many points of measurements are sufficient to estimate the deep profile mean soil water content of a hillslope in the Loess Plateau? Geoderma 314, 85–94. https://doi.org/10.1016/j.geoderma.2017.11.013.

Zhang, Y.W., Deng, L., Yan, W.M., Shangguan, Z.P., 2016. Interaction of soil water storage dynamics and long-term natural vegetation succession on the Loess Plateau, China. Catena 137, 52–60. https://doi.org/10.1016/j.catena.2015.08.016.

Zhao, S.W., Zhao, Y.G., Wu, J.S., 2010. Quantitative analysis of soil pores under natural vegetation successions on the Loess Plateau. Sci. Earth Sci. 53, 617–625. https://doi.org/10.1007/s11430-010-0029-8.

Zhao, X.K., Li, Z.Y., Zhu, Q.K., Zhu, D.H., Liu, H.F., 2017. Climatic and drought characteristics in the loess hilly-gully region of China from 1957 to 2014. Plos One 12, 1–28. https://doi.org/10.1371/journal.pone.0178701.